Transp Porous Med (2013) 99:175–189
DOI 10.1007/s11242-013-0180-8

The Onset of Prandtl–Darcy–Prats Convection in a Horizontal Porous Layer

Emily Dodgson · D. Andrew S. Rees

Received: 28 March 2013 / Accepted: 14 May 2013 / Published online: 31 May 2013

Abstract We consider the effect of finite Prandtl–Darcy numbers of the onset of convection in a porous layer heated isothermally from below and which is subject to a horizontal pressure gradient. A dispersion relation is found which relates the critical Darcy–Rayleigh number and the induced phase speed of the cells to the wavenumber and the imposed Péclet and Prandtl–Darcy numbers. Exact numerical solutions are given and these are supplemented by asymptotic solutions for both large and small values of the governing nondimensional parameters. The classical value of the critical Darcy–Rayleigh number is $4\pi^2$, and we show that this value increases whenever the Péclet number is nonzero and the Prandtl–Darcy number is finite simultaneously. The corresponding wavenumber is always less than π and the phase speed of the convection cells is always smaller than the background flux velocity.

Keywords Porous media · Onset of convection · Linearized theory · Dispersion relation · Horizontal flow

List of Symbols

Variables

c	Specific heat, phase speed of convection cells
c_a	Acceleration coefficient scalar
$f(z)$	Reduced streamfunction
F	Dispersion relation
$g(z)$	Reduced temperature
$\mathbf{g}$	Gravity vector
H	Height of the layer
k	Wavenumber

E. Dodgson · D. A. S. Rees (✉)
Department of Mechanical Engineering, University of Bath, Bath BA2 7AY, UK
e-mail: D.A.S.Rees@bath.ac.uk

k_{m}	Thermal conductivity of the porous medium
K	Permeability
n	Iteration number
P	Pressure
Pd	Prandtl–Darcy number
Pe	Péclet number
$\mathrm{Pr_m}$	Prandtl number
Ra	Darcy–Rayleigh number
t	Time
T	Dimensional temperature
T_0	Dimensional temperature of lower boundary
T_1	Dimensional temperature of upper boundary
$\mathbf{v}$	Darcy velocity vector
x, y, z	Coordinate sysem; see Fig. 1

Greek Symbols

α_{m}	Thermal diffusivity of the porous medium
β	Volumetric coefficient of thermal expansion
γ	Reciprocal of the Prandtl–Darcy number
ΔT	$T_0 - T_1$
θ	Nondimensional temperature
μ	Dynamic viscosity
ρ_0	Density
σ	Heat capacity ratio
ψ	Nondimensional streamfunction

Superscript, Subscripts

$\hat{}$	Dimensional quantity
$\tilde{}$	Perturbation
$'$	Ordinary derivative with respect to z
c	Critical value
f	Fluid
m	Porous medium
1, 2, 3 . . .	Terms in an asymptotic expansion

1 Introduction

In this paper we consider the onset of convection within an infinite horizontal porous layer heated from below in the presence of a horizontal pressure gradient when the Prandtl–Darcy number is finite. The pressure gradient drives a uniform fluid flow along the layer. The finite Prandtl–Darcy number (more recently known as the Vadász number) means there is a delay in the response of the flow field to any temperature or pressure changes.

Prats (1966) considered the effect of horizontal fluid flow on convection in the classical Darcy–Bénard problem and demonstrated that the criterion for neutral stability is unchanged by the presence of the pressure gradient from those derived by Horton and Rogers (1945),

Lapwood (1948) and Rogers (1953). The underlying flow which is generated by the pressure gradient causes the convection cells to move along the layer with a phase speed which is precisely equal to the Darcy velocity. Thus the linear stability problem of Prats reduces to that of the zero-flow layer when the governing equations are transformed into a frame of reference which moves with the flow. In practice, this causes temperature and pressure oscillations at any given fixed point in space.

One recent paper by Rees and Mojtabi (2013) is an example of how other effects serve to reduce the cell phase speed from that given by the Darcy velocity of the background flow. These authors considered the same problem as Prats (1966) but with the addition of two identical solid conducting layers above and below the porous layer. It was found that the presence of the stationary plates causes a thermal drag which serves to inhibit cell movement along the layer. However, we note that when Local Thermal Nonequilibrium effects are present, then it is possible for phase speeds to be larger than that of the background flow; a hint that this is possible is provided in Rees et al. (2008), but work in progress by one of the present authors shows that this is true in the Darcy–Bénard context.

The Prandtl–Darcy number is almost always taken to be infinite resulting in the neglect of the time derivative terms in Darcy's Law. However, as more detailed modellings of flows in porous media have been undertaken, it has been noted that this assumption is not always valid for modern applications; see, for example binary alloys where $\mathrm{Pr_m} \approx 100$ (Vadász and Olek 1999). The inclusion of these terms can effect the stability properties of convective flows in a porous layer. Work such as that described in Vadász and Olek (2000, 1999) has shown that the inclusion of these terms can affect the stability properties of convective flows in a porous layer when within the nonlinear regime, although the fact that the onset of Darcy–Bénard convection is stationary means that it is unaffected by the value of the Prandtl–Darcy number.

We have seen that the separate effects of finite Prandtl–Darcy numbers and nonzero Péclet numbers do not affect the onset criterion for convection in a porous layer. It is, therefore, the aim of the present paper to determine how these effects combine to alter the onset criterion. We derive a relationship between the Darcy–Rayleigh number and the wavenumber of transverse convection cells, and neutral curves are presented. Critical values are then found by minimising the Darcy–Rayleigh number with respect to the wavenumber, and the variations in these quantities are presented as functions of both the Prandtl–Darcy number and the background flow Péclet number. Asymptotic analyses are also undertaken for both small and large values of each nondimensional parameter. Of particular note is the fact that the critical wavenumber becomes of $O(\mathrm{Pe}^{-1/2})$ as the Péclet number, Pe, becomes asymptotically large, and the critical Darcy–Rayleigh number is then of $O(\mathrm{Pe}^2)$.

2 Governing Equations

We investigate the onset of convection in a fully saturated porous layer as shown in Fig. 1. When $T_0 > T_1$ the layer is unstably stratified and convective motion may occur. We assume that the medium is homogeneous and isotropic, that Darcy's law is valid, that the Oberbeck–Boussinesq approximation is applicable and that the phases are in local thermal equilibrium. The governing equations for flow in a saturated porous layer are now given by Nield and Bejan (2006) and may be written in the form,

$$\nabla \cdot \hat{\mathbf{v}} = 0, \tag{1}$$

$$c_a \rho_0 \frac{\partial \hat{\mathbf{v}}}{\partial \hat{t}} = -\nabla \hat{P} - \frac{\mu}{K}\hat{\mathbf{v}} + \rho_0 \mathbf{g}\beta(\hat{T} - T_0), \tag{2}$$

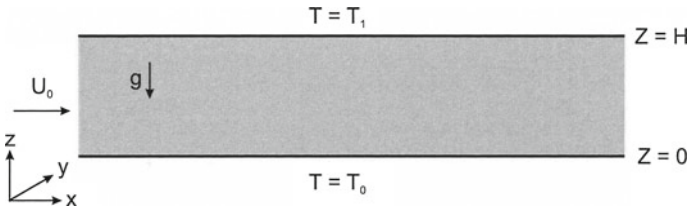

Fig. 1 A porous layer heated from below and subject to an imposed horizontal flow

$$(\rho c)_{\mathrm{m}} \frac{\partial \hat{T}}{\partial \hat{t}} + (\rho c_P)_f \hat{\mathbf{v}} \cdot \nabla \hat{T} = k_{\mathrm{m}} \nabla^2 \hat{T}. \tag{3}$$

The value, c_a, could generally be a tensorial quantity, but for an isotropic medium it may be regarded as a constant scalar which depends on the geometry of the porous medium, and which then governs how quickly velocity transients decay after a sudden change in pressure gradient or temperature. Thus relatively small pores admit a quicker transient decay than would arise in a material with larger pores but the same porosity (Nield and Bejan 2006).

The following scalings are introduced in order to nondimensionalise the governing equations,

$$\begin{gathered}(\hat{x}, \hat{y}, \hat{z}) = H(x, y, z), \quad \hat{\mathbf{v}} = \frac{\alpha_{\mathrm{m}}}{H}\mathbf{v}, \\ \hat{P} = \frac{\alpha_{\mathrm{m}}\mu}{K} P, \quad \hat{t} = \frac{\sigma H^2}{\alpha_{\mathrm{m}}} t, \quad \hat{T} = \theta \Delta T + T_0.\end{gathered} \tag{4}$$

Following Nield and Bejan (2006), we define the thermal diffusivity and the heat capacity ratio, respectively, by

$$\alpha_{\mathrm{m}} = \frac{k_{\mathrm{m}}}{(\rho c_P)_f}, \quad \sigma = \frac{(\rho c)_{\mathrm{m}}}{(\rho c_P)_f}. \tag{5}$$

Substitution of the identities given in (4) into Eqs. (1–3) gives

$$\nabla . \mathbf{v} = 0, \tag{6}$$

$$\gamma \frac{\partial \mathbf{v}}{\partial t} + \mathbf{v} = -\nabla P + \mathrm{Ra}\, \theta\, \mathbf{k}, \tag{7}$$

$$\frac{\partial \theta}{\partial t} + \mathbf{v} \cdot \nabla \theta = \nabla^2 \theta, \tag{8}$$

subject to the boundary conditions of $\theta = 1$ at $z = 0$ and $\theta = 0$ at $z = 1$ and of a zero flow perpendicular to the bounding surfaces. Two of the three nondimensional parameters which govern the dynamics of convection, the Darcy–Rayleigh number and the Prandtl–Darcy number, are defined, respectively, as

$$\mathrm{Ra} = \frac{\rho_0 g \beta K H \Delta T}{\mu \alpha_{\mathrm{m}}}, \quad \mathrm{Pd} = \frac{\sigma \mathrm{Pr}_{\mathrm{m}} H^2}{c_a K}, \tag{9}$$

where the Prandtl number is

$$\mathrm{Pr}_{\mathrm{m}} = \frac{\mu}{\rho_0 \alpha_{\mathrm{m}}}. \tag{10}$$

For convenience we will work with the reciprocal of the Prandtl–Darcy number:

$$\gamma = \mathrm{Pd}^{-1} = \frac{c_a K}{\sigma \mathrm{Pr}_{\mathrm{m}} H^2}, \tag{11}$$

and, therefore, zero values of γ correspond to the absence of a time derivative in Darcy's law.

The speed at which transients decay now depends on the value of γ. Generally, the value of γ is taken to be zero, which means that the fluid velocity adjusts instantaneously to changes in pressure gradient or temperature. The time derivative also needs to be retained in cases where wave effects are of interest in order to prevent the reduction of the order of the system in the time domain (Vadász and Olek 2000). It also needs to be retained when considering the effects of g-jitter on convection, particularly when the porous medium is in a microgravity environment and the jitter is caused by the normal operation of the spacecraft (Razi et al. 2009).

Before embarking on a detailed stability analysis it is of interest to determine the possible values that might be taken by the Prandtl–Darcy number. Vadász and Olek (2000) point out that $\mathrm{Pr_m}$ may take values in the range 10^{-3} for liquid metals to 10^{3} for oils, which, when multiplied by the other terms which are present in the definition of γ, gives rise to values of γ which are in the range 10^{2}–10^{-23}. The value $\gamma = 0.01$ has been said to describe the solidification of binary alloys (Vadász and Olek 2000). Thus the retention of the time derivative in Darcy's law does have significant application.

In this paper we restrict our attention to two-dimensional convection and define the stream-function defined according to,

$$u = -\frac{\partial \psi}{\partial z}, \quad v = 0, \quad w = \frac{\partial \psi}{\partial x}; \tag{12}$$

the governing equations become,

$$\left(1 + \gamma \frac{\partial}{\partial t}\right)\left[\frac{\partial^2 \psi}{\partial x^2} + \frac{\partial^2 \psi}{\partial z^2}\right] = \mathrm{Ra}\frac{\partial \theta}{\partial x}, \tag{13}$$

$$\frac{\partial \theta}{\partial t} - \frac{\partial \psi}{\partial z}\frac{\partial \theta}{\partial x} + \frac{\partial \psi}{\partial x}\frac{\partial \theta}{\partial z} = \nabla^2 \theta. \tag{14}$$

A horizontal pressure gradient is applied to the porous layer yielding the uniform dimensional velocity, U_0, in the x-direction, as shown in Fig. 1. Therefore, the boundary conditions for ψ may be taken to be $\psi = \mathrm{Pe}/2$ at $z = 0$ and $\psi = -\mathrm{Pe}/2$ at $z = 1$, where the Péclet number is defined according to

$$\mathrm{Pe} = \frac{H U_0}{\alpha_\mathrm{m}}, \tag{15}$$

and the Péclet number may, therefore, be regarded as being the nondimensional Darcy velocity along the layer.

3 Linear Perturbation Analysis

The basic steady-state solution to Eqs. (13–14) is

$$\theta = 1 - z, \quad \psi = -\mathrm{Pe}\left(z - \tfrac{1}{2}\right). \tag{16}$$

The linear perturbation analysis proceeds by letting

$$\theta = 1 - z + \tilde{\theta}, \quad \psi = -\mathrm{Pe}\left(z - \tfrac{1}{2}\right) + \tilde{\psi}. \tag{17}$$

which upon substitution into Eqs. (13–14) gives

$$\left(1+\gamma\frac{\partial}{\partial t}\right)\left(\frac{\partial^2\tilde{\psi}}{\partial x^2}+\frac{\partial^2\tilde{\psi}}{\partial z^2}\right)=\mathrm{Ra}\frac{\partial\tilde{\theta}}{\partial x}, \tag{18}$$

$$\frac{\partial\tilde{\theta}}{\partial t}+\mathrm{Pe}\frac{\partial\tilde{\theta}}{\partial x}-\frac{\partial\tilde{\psi}}{\partial x}=\nabla^2\tilde{\theta}. \tag{19}$$

We let

$$\tilde{\psi}=\mathrm{Real}\left[f(z)e^{ik(x-ct)}\right],\quad \tilde{\theta}=\mathrm{Real}\left[-ig(z)e^{ik(x-ct)}\right]. \tag{20}$$

Putting the definitions of (20) into Eqs. (18–19) gives;

$$(1-i\gamma kc)(f''-k^2f)=\mathrm{Ra}\,kg, \tag{21}$$

$$g''-k^2g=kf-ikg(c-\mathrm{Pe}). \tag{22}$$

This system is simplified further by setting,

$$f=A\sin(\pi z),\quad g=B\sin(\pi z) \tag{23}$$

in Eqs. (21–22). We take both Ra and the phase speed, c, to be purely real. Elimination of the constants A and B yields the dispersion relation,

$$\mathrm{Ra}\,k^2-\left(1-i\gamma kc\right)\left(k^2+\pi^2\right)\left(k^2+\pi^2+ik(\mathrm{Pe}-c)\right)=0. \tag{24}$$

The imaginary part of this equation yields

$$c=\frac{\mathrm{Pe}}{1+(\pi^2+k^2)\gamma} \tag{25}$$

and the substitution of this into the real components gives

$$\mathrm{Ra}=\frac{(\pi^2+k^2)^2}{k^2}+\frac{\gamma^2\mathrm{Pe}^2(\pi^2+k^2)^2}{(1+\gamma(\pi^2+k^2))^2}. \tag{26}$$

We note that the setting of either $\gamma=0$ or $\mathrm{Pe}=0$ leads to the recovery of the traditional Darcy–Bénard onset criterion as derived by Horton and Rogers (1945), Lapwood (1948) and Rogers (1953) for which the neutral curve is,

$$\mathrm{Ra}=\frac{(k^2+\pi^2)^2}{k^2}. \tag{27}$$

This has a minimum at $\mathrm{Ra}_c=4\pi^2$ at which point $k_c=\pi$. When $\gamma=0$ then $c=\mathrm{Pe}$ and the cells move at a phase speed which is equal to the background flow, as shown first by Prats (1966). For general nonzero values of both γ and Pe, it is very clear from Eqs. (25–26) that the critical Darcy–Rayleigh number must be higher than $4\pi^2$ and that the phase speed of the cells is less than the value of Pe.

4 Numerical Method

While Ra is given explicitly in terms of k and the nondimensional parameters, Pe and γ, and, therefore, it is straightforward to plot neutral curves, the minimisation of Ra with respect to

k cannot be undertaken analytically. Therefore, we use a two-dimensional Newton–Raphson scheme to achieve this. At a minimum in the neutral curve we set,

$$F(\mathrm{Ra}, k) = \mathrm{Ra} - \frac{(\pi^2 + k^2)^2}{k^2} - \frac{\gamma^2 \mathrm{Pe}^2 (\pi^2 + k^2)^2}{(1 + \gamma(\pi^2 + k^2))^2} = 0, \tag{28}$$

$$\frac{\partial F}{\partial k} = 0. \tag{29}$$

These definitions give the iteration scheme:

$$\begin{pmatrix} \mathrm{Ra}_{n+1} \\ k_{n+1} \end{pmatrix} = \begin{pmatrix} \mathrm{Ra}_n \\ k_n \end{pmatrix} - \begin{pmatrix} \dfrac{\partial F}{\partial \mathrm{Ra}} & \dfrac{\partial F}{\partial k} \\ \dfrac{\partial^2 F}{\partial k \partial \mathrm{Ra}} & \dfrac{\partial^2 F}{\partial k^2} \end{pmatrix}^{-1} \begin{pmatrix} F \\ \dfrac{\partial F}{\partial k} \end{pmatrix} \tag{30}$$

where the subscript n denotes the iteration number; this method has also been used successfully in the recent papers by Rees and Genç (2011) and Genç and Rees (2011). Two entries the matrix are simple to evaluate analytically:

$$\frac{\partial F}{\partial \mathrm{Ra}} = 1 \quad \text{and} \quad \frac{\partial^2 F}{\partial k \partial \mathrm{Ra}} = 0. \tag{31}$$

5 Results and Asymptotic Analyses

In this section we will present some neutral curves and give a comprehensive overview of the stability properties of the system. Four different asymptotic analyses are presented briefly, and these correspond to asymptotically large and small values of both Pe and γ.

5.1 Neutral Curves

The numerical scheme outlined in the previous section allows the calculation of the critical values of Ra and k for a large range of values of Pe and γ. We note that, given the form of the above dispersion relation, it is necessary for both Pe and γ to be nonzero for the neutral curve to change from that of the classical Darcy–Bénard problem. Typical neutral curves for fixed values of Pe and γ are shown in Figs. 2 and 3.

The subfigures contained in Fig. 2 show how variations in Pe affect the neutral curves when $\gamma = 0.01$ and $\gamma = 10$. These neutral curves represent the general case by being unimodal and where $\mathrm{Ra} \to \infty$ as $k \to 0$ and $k \to \infty$. When $\gamma = 0.01$ the response of the flow field to changes in the temperature field is very quick. Therefore, it requires quite a strong background flow to be imposed before the neutral curves begin to change from that of the classical Darcy–Bénard problem, which is represented here by the $\mathrm{Pe} = 0$ curve. As the Péclet number increases the critical Darcy–Rayleigh number also increases but the critical wavenumber decreases. This means that the flow is increasingly stable and that the wavelength of the most dangerous disturbance increases. This appears to be physically reasonable: even though the flow field adjusts quickly to changes in the temperature, there will come a point where the background flow is too fast for the flow to adjust. Therefore, it is essential that the buoyancy effects have to become stronger in order to attain instability, and hence an increased value of Ra is necessary. In addition, when cells have a long wavelength, then the time it takes for one cell to pass a fixed location means that there is a larger time

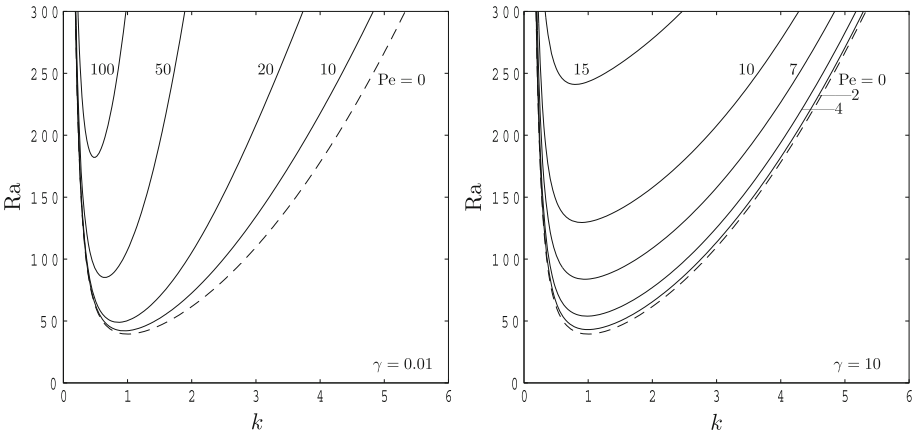

Fig. 2 Neutral curves for $\gamma = 0.01$ and $\gamma = 10$, and for various values of Pe

available for the flow field to respond than there would be for a smaller wavelength cell. Thus it is to be expected that the critical wavenumber will decrease from π.

A similar behaviour is found in Fig. 2b, for which $\gamma = 10$. Once more the critical value of Ra increases and of k decreases as Pe increases, but they do so much more rapidly as Pe increases. For example, when $\gamma = 0.01$ and $\mathrm{Pe} = 100$, the critical value of Ra is close to 200. When γ has increased to 10, a similar value of Ra_c is obtained when $\mathrm{Pe} \simeq 12$, a much smaller background flow strength. This change is caused by the fact that larger values of γ naturally reduce the ability of flow field to react to changes in θ.

It is important to note that the critical Darcy–Rayleigh number continues to rise indefinitely and the corresponding wavenumber to reduce towards zero as the Péclet number increases; the precise way in which this happens is dealt with below.

In Fig. 3 we present three sets of neutral curves showing how they vary with increasing γ for $\mathrm{Pe} = 5$, 10 and 20. The act of continuing to increase γ for fixed values of Pe does not give exactly the same change in the behaviour of the neutral curves as was seen in Fig. 2 where γ was fixed and Pe increases. In all three cases shown in Fig. 3 we see that, while the curves generally rise vertically as γ increases, they all tend towards a limiting curve as $\gamma \to \infty$. When Pe takes small values, then there is little change between the small-γ curves and the large-γ curves. That this should be so may be understood by appealing to the fact that the background flow is weak, and, therefore, we are in a situation where the onset of convection is quasi-static and, therefore, almost independent of γ.

For larger values of Pe such as 10 and 20, which correspond, respectively, to Figs. 3b and c, an ever-increasing gap is formed between the small-γ limiting curve and the large-γ limiting curve. As γ increases the critical wavenumber decreases at first but then increases once more back towards π. This is seen more clearly in Fig. 3c than for the other two cases.

5.2 Critical Points

Given that the first mode to appear as Ra increases is the one corresponding to the minimum in the neutral curve, we now concentrate on such critical points and how they vary with Pe and γ. Figures 4, 5 and 6 depict in turn the critical Darcy–Rayleigh number, the corresponding wavenumber and phase speed. For convenience of presentation, and in particular because the

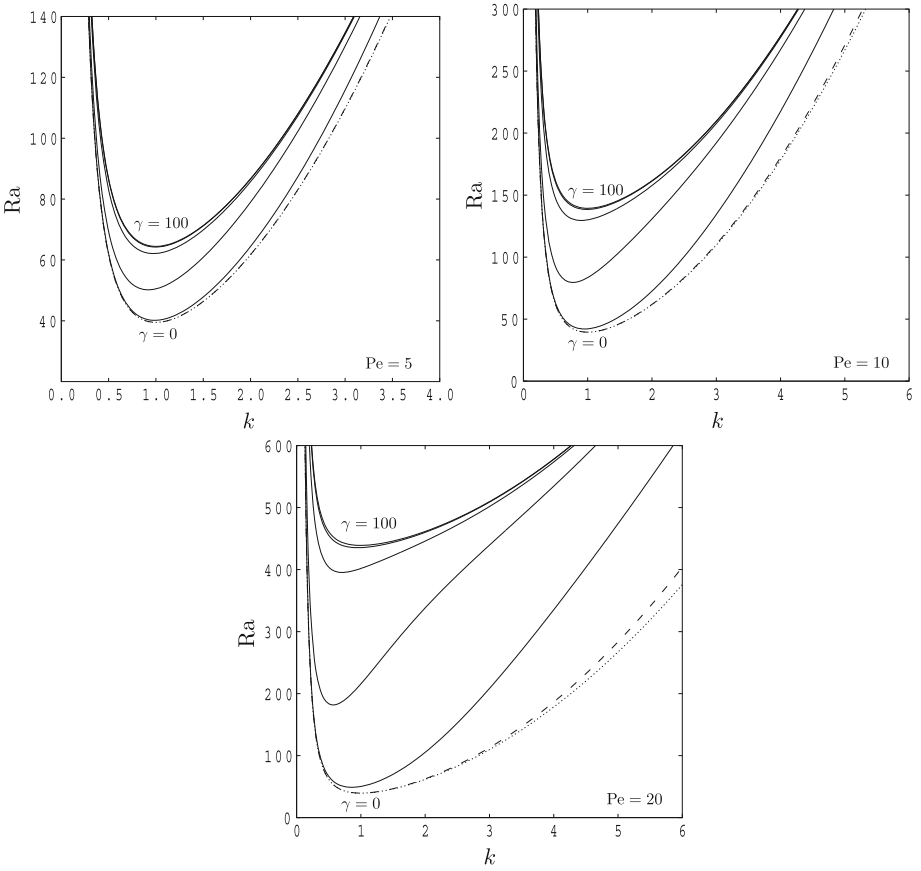

Fig. 3 Neutral curves for Pe = 5, 10 and 20. The following values of γ have been used: 0 (*dotted line*), 10^{-3} (*dashed line*), 10^{-2}, 10^{-1}, 10^{0}, 10^{1} and 10^{2}

critical Darcy–Rayleigh number varies over many orders of magnitude as Pe varies, these quantities have been scaled.

Figure 4 shows contours of $\log_{10}(\mathrm{Ra}_c/4\pi^2)$ over a wide range of values of Pe and γ. It is important to note the contour levels in this Figure. Those to the right of the thick line have values which increase linearly in $\log_{10}(\mathrm{Ra}_c/4\pi^2)$ while those on the left increase exponentially from very small values as Pe increases.

When Pe and γ take small values, the critical Darcy–Rayleigh number is very close to $4\pi^2$. But for all values of γ, Ra_c increases strongly as Pe increases. In fact, the asymptotic analyses in §§5.3 and 5.4 show that Ra_c increases as a power of Pe^2 when $\mathrm{Pe} \ll 1$ and when $\mathrm{Pe} \gg 1$, although the constant of proprtionality is different in the two regimes.

There are two distinct regimes within Fig. 4 and they correspond essentially to the upper and lower halves as depicted. In the upper half the value of Ra_c is independent of γ, and this is confirmed by the asymptotic analysis in §5.6. In the lower half, the contour lines suggest clearly that Ra_c depends at leading order on the ratio, Pe/γ. Although we do not present an analysis of this scenario, i.e. one where both parameters vary, it represents a case when Pe is large (for which the background flow is strong) and γ is small (for which

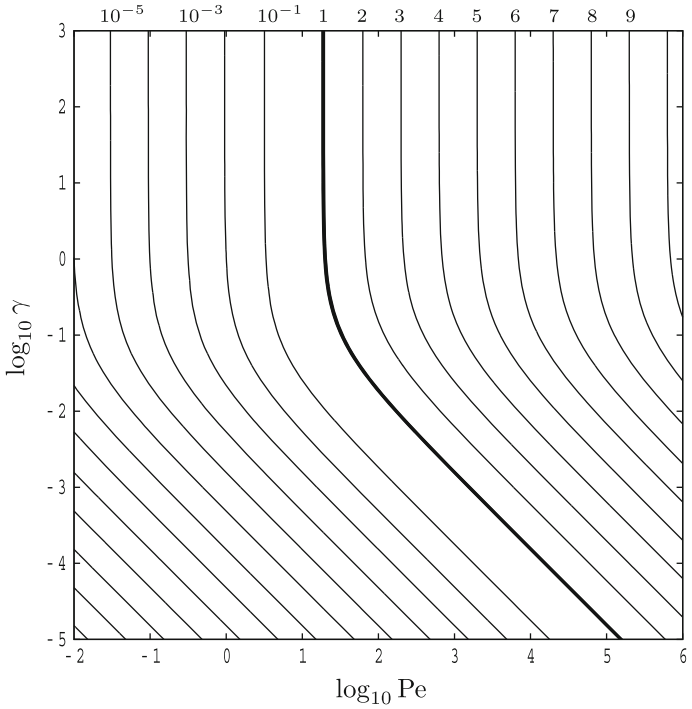

Fig. 4 Contours of $\log_{10}(\mathrm{Ra}_c/4\pi^2)$ as a function of $\log_{10}\mathrm{Pe}$ and $\log_{10}\gamma$. The contour values are given at the *top* of the figure. The *thick line* represents $\mathrm{Ra}_c = 400\pi^2$. Contour values to the *left* of the *thick line* decrease by factors of 10

the speed of response of the flow field is rapid). Thus it represents a further distinguished limit.

From the data it is clear that Ra_c is within 10 % of $4\pi^2$ (i.e. $\log_{10}\mathrm{Ra}_c/4\pi^2 < 0.0414$) when Pe takes values less than roughly 1 for all values of γ.

Figure 5 shows the corresponding contours for the critical wavenumber in the form, k_c/π. Our earlier observation that the critical wavenumber decreases as the Péclet number increases is shown here quite clearly. On the other hand, the slightly more complicated behaviour of the critical wavenumber which was seen in Fig. 3, where it at first decreases and then increases once more as γ increases, is shown to be a universal phenomenon. In all cases k_c decreases from π and then increases back to π, which is also seen in the asymptotic expansions given in §§5.5 and 5.6. We may also state that k_c is within 10 % of π whenever Pe is less than roughly 8.

Figure 6 shows how c/Pe varies. This is a scaled phase velocity and has been used in order make the dependence on Pe and γ clearer. This scaled phase speed is a strongly varying function of γ, which, given its role in determining the speed of reaction of the flow to changing thermal conditions, is not surprising. It is, on the one hand, only weakly dependent on Pe. The asymptotic analyses in the next four subsections yield the following expressions for the phase speed:

$$c/\mathrm{Pe} \sim \frac{1}{1+2\pi^2\gamma} \quad (\mathrm{Pe} \ll 1), \qquad c/\mathrm{Pe} \sim \frac{1}{1+\pi^2\gamma} \quad (\mathrm{Pe} \gg 1), \tag{32}$$

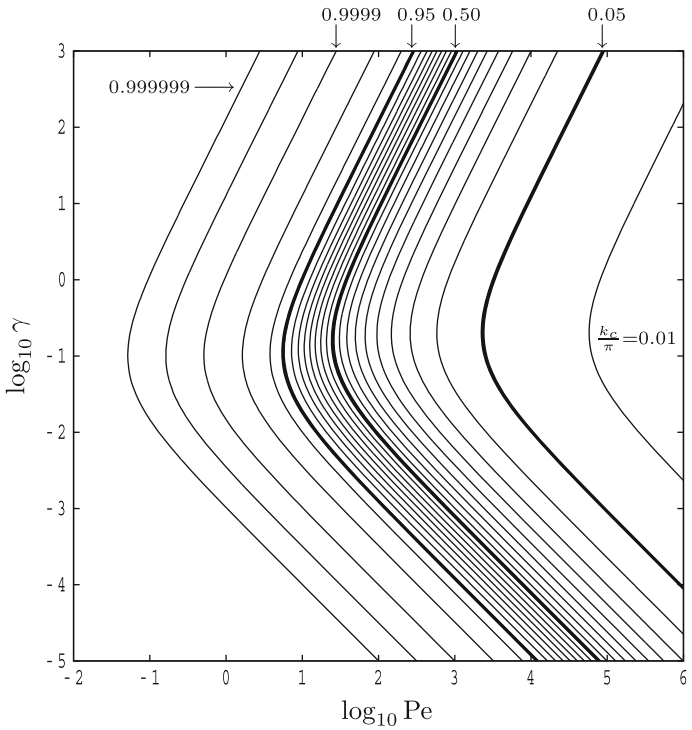

Fig. 5 Contours of k_c/π as a function of $\log_{10}\mathrm{Pe}$ and $\log_{10}\gamma$. The contour values are given at the *top* and *within* the figure. Contour values to the *left* of the $k_c/\pi = 0.95$ *line* correspond to 0.99, 0.999, 0.9999 and so on

and

$$c/\mathrm{Pe} \sim 1 - \pi^2\gamma, \quad (\gamma \ll 1), \qquad c/\mathrm{Pe} \sim \frac{1}{2\pi^2\gamma}, \quad (\gamma \gg 1). \tag{33}$$

All of these may be seen in Fig. 6, including the very slight change in the value of c/Pe which may be seen as Pe increases and which is associated with the boomerang-shaped region of rapid changes in the critical wavenumber shown in Fig. 5.

5.3 Asymptotic Analysis for $\mathrm{Pe} \ll 1$

In this first asympotic analysis we investigate the regime where the background flow is extremely weak. On setting $\epsilon = \mathrm{Pe}^2$, we expand k and Ra in powers of ϵ:

$$\begin{aligned} k &= \pi(1 + \epsilon k_1 + \epsilon^2 k_2) + O(\epsilon^3), \\ \mathrm{Ra} &= 4\pi^2 + \epsilon \mathrm{Ra}_1 + \epsilon^2 \mathrm{Ra}_2 + O(\epsilon^3), \end{aligned} \tag{34}$$

and substitute into Eq. (26). Equating terms of $O(\epsilon)$ we obtain

$$\mathrm{Ra}_1 = \frac{4\pi^2\gamma^2}{(1 + 2\pi^2\gamma)^2}. \tag{35}$$

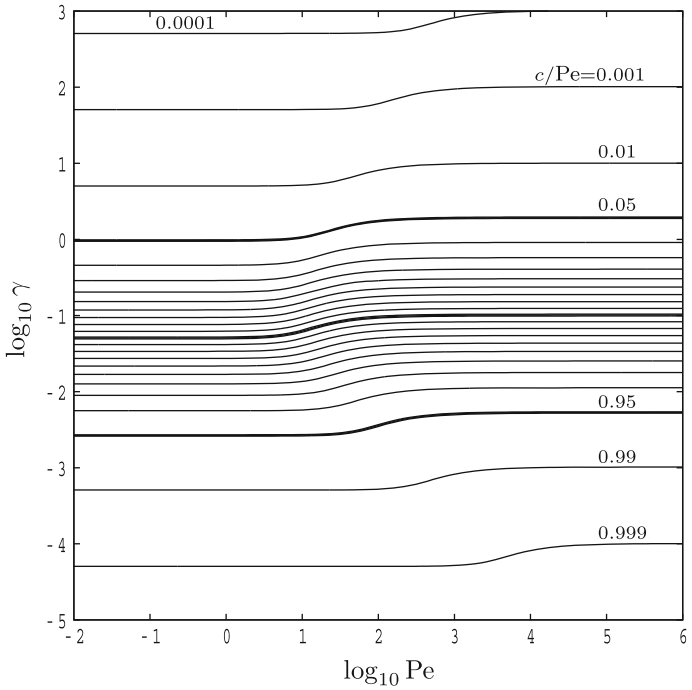

Fig. 6 Contours of c/Pe as a function of $\log_{10}\mathrm{Pe}$ and $\log_{10}\gamma$. The contour values between the outer *thick lines* are at equally spaced intervals

At $O(\epsilon^2)$ we derive

$$\mathrm{Ra}_2 = 4\pi^2 k_1^2 + \frac{8\pi^4\gamma^2 k_1}{(1+2\pi^2\gamma)^3}, \tag{36}$$

which is minimised for when the gradient with respect to k_1 is zero giving;

$$k_1 = -\frac{\pi^2\gamma^2}{(1+2\pi^2\gamma)^3}. \tag{37}$$

Table 1 compares values produced by the Newton–Raphson scheme with those given by the asymptotic values for a range of γ and Pe. It shows an excellent correlation between both methods for all values of γ for $\mathrm{Pe} \leq 1$. Agreement for Ra_c remains reasonable to $\mathrm{Pe} = 10$, but has deteriorated for k_c. Given that we have approximated Ra to $O(\epsilon^2)$ and k to $O(\epsilon)$ this is perhaps to be expected. It is interesting to note that k_c is independent of Pe to 8 significant figures according to the small Pe analysis.

For small Péclet numbers it is now straightforward to show that the leading order behaviour of the phase velocity is given by,

$$c \sim \frac{Q}{1+2\pi^2\gamma}, \tag{38}$$

which shows that the value of γ remains a strong influence on the movement of the cells.

Table 1 Comparison of numerical and small Pe analysis Ra_c and k_c

Pe	γ	$\frac{\mathrm{Ra}_c - 4\pi^2}{\mathrm{Pe}^2}$		$\frac{k_c - \pi}{\mathrm{Pe}^2}$	
		Numerical	Small Pe analysis	Numerical	Small Pe analysis
0.01	0.01	0.02717607	0.02717607	−0.00180743	−0.00180609
0.01	0.1	0.44055548	0.44055548	−0.01178853	−0.01178858
0.01	1.0	0.90588926	0.90588926	−0.00347130	−0.00347595
1.0	0.01	0.02716304	0.02716303	−0.00180298	−0.00180610
1.0	0.1	0.44000175	0.43999965	−0.01172204	−0.01178858
1.0	1.0	0.90584095	0.90584094	−0.00347346	−0.00347595
10.0	0.01	0.02603042	0.02587128	−0.00154919	−0.00180609
10.0	0.1	0.40117425	0.03849673	−0.00723282	−0.01178858
10.0	1.0	0.90118571	0.90105639	−0.00318519	−0.00347595

5.4 Asymptotic Analysis for $\mathrm{Pe} \to \infty$

We now investigate the situation when $\mathrm{Pe} \to \infty$, which corresponds to when the speed of the background flow is large. The numerical data suggest the following forms for k and Ra:

$$k = \frac{k_1}{\sqrt{\mathrm{Pe}}} + \frac{k_2}{\mathrm{Pe}} + O(\mathrm{Pe}^{-3/2}), \tag{39}$$

$$\mathrm{Ra} = \mathrm{Pe}^2\,\mathrm{Ra}_1 + \mathrm{Pe}\,\mathrm{Ra}_2 + O(1). \tag{40}$$

Substituting these into Eq. (26) gives

$$\mathrm{Ra}_1 = \frac{\gamma^2\pi^4}{(1+\gamma\pi^2)^2} \tag{41}$$

at $O(\mathrm{Pe}^2)$. At $O(\mathrm{Pe})$ we find

$$\mathrm{Ra}_2 = \frac{\pi^4}{k_1^2} + \frac{2\pi^2\gamma^2 k_1^2}{(1+\gamma\pi^2)^3} \tag{42}$$

$$k_1 = \left(\frac{\pi^2(1+\gamma\pi^2)^3}{2\gamma^2}\right)^{\frac{1}{4}}, \tag{43}$$

where the given value of k_1, and hence of Ra_2, is that which minimises the expression for Ra_2 in Eq. (42). Higher order analysis yields $k_2 = 0$. The leading order expression for the phase speed is given,

$$c \sim \frac{\mathrm{Pe}}{1+\pi^2\gamma}. \tag{44}$$

Table 2 compares the numerical and asymptotic results for Ra_c and k_c to 8 significant figures. Agreement is outstanding at $\mathrm{Pe} = 7{,}000$, and we would only expect this to improve as Pe increases although the limitations of the numerical method prevent us investigating this further. The large-Pe relationship is shown to still provide a reasonable order-of-magnitude estimation as low as $\mathrm{Pe} = 2{,}000$.

Table 2 Comparison of numerical and large-Pe analysis: values of Ra_c and k_c

Pe	γ	Ra_c		k_c	
		Numerical	Large Pe analysis	Numerical	Large Pe analysis
2,000	0.01	33,824.307	33,800.862	0.35680276	0.35765196
5,000	0.01	205,567.41	205,544.03	0.22598453	0.22619896
7,000	0.01	400,757.42	400,734.05	0.19104361	0.19117301
2,000	1.0	3,302,764.1	3,302,752.9	0.19985600	0.19950912
5,000	1.0	20,623,862	20,623,851	0.12626838	0.12618064
7,000	1.0	40,415,907	40,415,896	0.10669507	0.10664211

5.5 Asymptotic Analysis for $\gamma \ll 1$

We turn our attention to the stability of the system as $\gamma \to 0$, that is as the Prandtl–Darcy number increases and the flow field responds more quickly to any disturbance. In this case we expand k and Ra in a simple power series in γ:

$$(\mathrm{Ra}, k) = \sum_{n=0} (\mathrm{Ra}_n, k_n)\gamma^n, \tag{45}$$

where the summation is over positive integers. Equation (26) gives $\mathrm{Ra}_1 = 0$ at $O(\gamma)$. At $O(\gamma^2)$ we obtain $k_1 = 0$ and $\mathrm{Ra}_2 = 4\pi^4\mathrm{Pe}^2$. Equating terms at $O(\gamma^3)$ gives $\mathrm{Ra}_3 = -16\pi^6\mathrm{Pe}^2$. Finally the terms at $O(\gamma^4)$ give,

$$\mathrm{Ra}_4 = 4\pi^2 k_2^2 + 4\pi^4\mathrm{Pe}^2(2k_2 + 12\pi^4), \tag{46}$$

which is minimised when its derivative with respect to k_2 is zero, giving $k_2 = -\pi^2\mathrm{Pe}^2$. Consequently the critical values of Ra and k are calculated to be,

$$k = \pi(1 - \gamma^2\pi^2\mathrm{Pe}^2) \tag{47}$$

$$\mathrm{Ra} = 4\pi^2\Big[1 + \gamma^2\pi^2\mathrm{Pe}^2 - \gamma^3 4\pi^4\mathrm{Pe}^2 + \gamma^4\Big(48\pi^8 - 8\pi^6\mathrm{Pe}^2\Big)\Big]. \tag{48}$$

We may now find the leading behaviour of the phase speed:

$$c \sim \mathrm{Pe}(1 - \pi^2\gamma). \tag{49}$$

Hence cells travel at very close to the speed of the background flow, which is to be expected given that the flow adjusts very quickly to changing thermal conditions when γ is small.

5.6 Asymptotic Analysis for $\gamma \to \infty$

This asymptotic limit is unlikely to correspond to a physical system, but it is nevertheless of some mathematical interest. The analysis is very similar in style to the large-Pe analysis above and, therefore, simply summarise the final result. When $\gamma \gg 1$ the critical point of the curve given by Eq. (26) may be found to be given by the following:

$$k_c = \pi - \Big(\frac{\mathrm{Pe}^2}{16\pi^3}\Big)\gamma^{-1} + O(\gamma^{-2}) \tag{50}$$

$$\mathrm{Ra}_c = \Big(4\pi^2 + \mathrm{Pe}^2\Big) - \Big(\frac{\mathrm{Pe}^2}{\pi^2}\Big)\gamma^{-1} + \Big(\frac{\mathrm{Pe}^2}{4\pi^4} - \frac{\mathrm{Pe}^6}{64\pi^6}\Big)\gamma^{-2} + O(\gamma^{-3}). \tag{51}$$

The corresponding phase speed for the cells is

$$c \sim \frac{\mathrm{Pe}}{2\pi^2}\gamma^{-1}, \tag{52}$$

and, therefore, the large-γ limit yields almost stationary cells.

6 Conclusion

A linear perturbation analysis has been carried out for a fully saturated porous layer, heated from below, subject to a uniform and steady horizontal pressure gradient and a finite Prandtl–Darcy number. The dynamics of the onset problem are governed by the two nondimensional parameters, Pe and γ, which are the nondimensional background flow and the reciprocal of the Prandtl–Darcy number, respectively. When either or both of these parameters are zero, then the onset condition for convection is identical to that obtained by Horton and Rogers (1945), Lapwood (1948) and Rogers (1953). However, when both parameters are nonzero then they interact, and generally the critical value of Ra is larger than $4\pi^2$ and the wavenumber is smaller than π. A comprehensive set of numerical (though exact) results have been presented for the critical Darcy–Rayleigh number and the corresponding wavenumber and cell phase speed. Extreme cases have been analysed using asymptotic analyses.

Whenever $\gamma \neq 0$ the critical Darcy–Rayleigh number increases with Péclet number and the wavenumber decreases. On the other hand, when $\mathrm{Pe} \neq 0$, the value of Ra_c increases with γ and then tends to a constant value as γ increases. At the same time wavenumber at first decreases from π and then increases back towards π, while phase speed of the cells relative to the strength of the background flow decreases towards zero.

References

Genç, G., Rees, D.A.S.: The onset of convection in horizontally partitioned porous layers. Phys. Fluids. **23**, 064107 (9 pp) (2011)
Horton, C.W., Rogers, F.T.: Convection currents in a porous medium. J. Appl. Phys. **16**, 367–370 (1945)
Lapwood, E.R.: Convection of a fluid in a porous medium. Proc. Camb. Philos. Soc. **4**, 508–521 (1948)
Nield, D.A., Bejan, A.: Convection in Porous Media, 3rd edn. Springer, New York (2006)
Prats, M.: The effect of horizontal fluid flow on thermally induced convection currents in porous mediums. J. Geophys. Res. **71**(20), 4835–4838 (1966)
Razi, Y.P., Mojtabi, A., Charrier-Mojtabi, M.C.: A summary of new predictive high frequency thermo-vibrational models in porous media. Transp. Porous Media **77**, 207–228 (2009)
Rees, D.A.S., Genç, G.: Onset of convection in porous layers with multiple horizontal partitions. Int. J. Heat Mass Transf **54**, 3081–3089 (2011)
Rees, D.A.S., Mojtabi, A.: The effect of conducting boundaries on Lapwood–Prats convection. Int. J. Heat Mass Transf. (2013)
Rees, D.A.S., Bassom, A.P., Siddheshwar, P.G.: Local thermal non-equilibrium effects arising from the injection of a hot fluid into a porous medium. J. Fluid Mech. **594**, 379–398 (2008)
Rogers, F.T.: Convection currents in porous media. V. Variational form of the theory. J. Appl. Phys. **24**, 877–880 (1953)
Vadász, P., Olek, S.: Weak turbulence and chaos for low Prandtl number gravity driven convection in porous media. Transp. Porous Media **37**, 69–91 (1999)
Vadász, P., Olek, S.: Route to chaos for moderate Prandtl number convection in a porous layer heated from below. Transp. Porous Media **41**, 211–239 (2000)